JOURNAL OF GUIDANCE, CONTROL, AND DYNAMICS
Vol. 17, No. 3, May–June 1994

Approximate Recovery of H_∞ Loop Shapes Using Fixed-Order Dynamic Compensation

Edward V. Byrns Jr.*
Systems Planning and Analysis, Inc., Falls Church, Virginia 22041
and
Anthony J. Calise†
Georgia Institute of Technology, Atlanta, Georgia 30332

This paper presents a method for designing fixed-order dynamic compensators that approximate the H_∞ full state feedback, closed-loop transfer function properties from disturbance inputs to controlled outputs. This formulation uses an observer canonical form to represent the dynamic compensator which allows the design to be treated as a modified constant gain output feedback problem. The approximate recovery is accomplished through a unique selection of the quadratic performance index weighting matrices. This design procedure is demonstrated by two design examples. The first example is a simple fourth-order model used to demonstrate the procedure. The second example is a longitudinal flight controller for the F-18/HARV "Supermaneuverable" aircraft. This flight controller is compared to both a full- and reduced-order H_∞ compensator.

Introduction

FIXED-ORDER dynamic compensators are a promising approach to designing low-order controllers. The compensator order is selected at the outset of the design, and this constraint is included in the derivation of the necessary conditions for optimality. However, in the past, this approach to compensator design has suffered from a lack of guarantees with respect to stability and performance robustness. In Ref. 1, a design technique is presented for approximately recovering linear quadratic regulator (LQR) properties at the plant input when implementing a fixed-order dynamic compensator in observer canonical form.[2] This formulation parallels the well-known loop transfer recovery (LTR) design technique.[3] Full state gains are first computed for desirable loop properties at the plant input, followed by the fixed-order compensator design to approximately recover these characteristics. It has also been shown in Ref. 4 that the approximate LTR formulation at the plant output is the exact dual of the procedure in Ref. 1. Similar to the observer-based LTR technique, these fixed-order dynamic compensator design methodologies approximately recover the loop properties at only the plant input or the plant output. They do not consider the problem of recovery of the transfer function properties from disturbances to controlled outputs.

A primary feature of H_∞ design (and its extension to μ synthesis for structured uncertainty) is that it achieves the desired effect of robust performance for disturbances and uncertainty occurring at multiple locations in the control loop. However, in the early development of H_∞ control, it was observed that the order of the H_∞ controller may be very large—much larger than the order of the design model. Recent research has concentrated on output feedback controllers that have the same dimension as that of the model.[5] In this case, it is possible to reduce the H_∞ design problem to the solution of a coupled set of Riccati equations. By repeated iteration of these Riccati equations, the H_∞ norm of the closed-loop transfer function from input disturbances to controlled outputs is reduced arbitrarily close to the optimal value.

A special case for H_∞ control design is to assume that all of the states are available as outputs. In this instance, the H_∞ controller reduces to a constant gain feedback design and constitutes the H_∞ analog of the LQR control problem.[5–7] The methodology requires the repeated solution of a single algebraic Riccati equation for decreasing values of an attenuation constant. This parameter is the upper bound for the H_∞ norm of the closed-loop transfer function. Therefore, robust performance can be accomplished with a constant gain full state feedback matrix.

In H_∞ design, the model order is determined by the plant dynamics plus all of the additional states required to introduce frequency weighting functions at the plant input and outputs. The model order is further increased by the frequency dependent D scaling required in the extension of H_∞ design to μ synthesis. These filters are essential to achieve the required loop shapes and become absorbed in what is referred to as the plant description. Thus, an H_∞ design produces the desired effect of robust performance but at the cost of a large increase in controller dimension. The order of the resulting full-order compensator may be too large for implementation purposes. Numerous methods are available to reduce the order of the compensator, but this process can lead to a suboptimal final design. The robustness gained by the H_∞ design can be lost in the subsequent controller-order reduction step since these two processes have different objectives.

An approach to designing fixed-order H_∞ controllers has been developed using the concept of optimal projection.[8,9] In this methodology, the dynamic compensator design is performed without a predetermined canonical structure. The necessary conditions reduce to a system of two modified Riccati equations and two modified Lyapunov equations coupled by a projection equation. The principal advantage in this form of the necessary conditions is that in the special case where the order of the compensator equals the order of the plant, the modified Riccati equations reduce to the standard equations. However, the system of equations are highly coupled and difficult to solve for the general case.

In the fixed-order compensator design approach presented here, all of the loop shaping needed to meet performance and robustness specifications is carried out in the context of full state feedback. A second step is then carried out to design a fixed-order compensator to approximately recover the closed-loop transfer function properties of the H_∞ full state design. This is accomplished by appropriately selecting the quadratic performance index weighting matrices and the variance of the initial condition distribution. Canonical forms are employed to represent the compensator dynamics, thus minimizing the dimension of the resulting parameter optimization problem. The main advantage here is that it may be simpler to solve these necessary conditions than the optimal projection equations.

Received July 2, 1991; presented as Paper 91-2729 at the AIAA Guidance, Navigation, and Control Conference, New Orleans, LA, Aug. 12–14, 1991; revision received May 22, 1993; accepted for publication July 20, 1993.

*Analyst, 5111 Leesburg Pike, Suite 200. Member AIAA.
†Professor, School of Aerospace Engineering. Fellow AIAA.

A brief outline of the paper is as follows. First, the observer canonical compensator form and the input approximate LTR design procedure are reviewed. The main contribution of the paper is contained in the next section, which analyzes the approximate recovery of the H_∞ closed-loop transfer function properties. This is followed by the methodology for the compensator design. The paper concludes with two example designs. The first example is a simple fourth-order model, taken from Ref. 7, which demonstrates this compensator design technique. The second example is a longitudinal flight controller for the F-18/HARV "Supermaneuverable" aircraft.[10,11] The resulting controller is compared to both a full- and reduced-order H_∞ compensator.

Fixed-Order Dynamic Compensators

Observer Canonical Form

In Ref. 2, a formulation based on an observer canonical structure was first presented for designing fixed-order dynamic compensators. The order of the compensator is first selected, and then its structure is determined by the choice of observability indices. This canonical form is reviewed subsequently.

Consider the standard linear multivariable system

$$\dot{x} = Ax + Bu \qquad x \in \Re^n, \quad u \in \Re^m \tag{1}$$

$$y = Cx + Du \qquad y \in \Re^p \tag{2}$$

which has the transfer function from u to y

$$G(s) = C\Phi B + D, \qquad \Phi = (sI - A)^{-1} \tag{3}$$

A compensator in observer canonical form for the system in Eqs. (1) and (2) can be described as

$$\dot{z}_{ob} = P^o_{ob} z_{ob} + u_o \qquad z_{ob} \in \Re^{nc} \tag{4}$$

$$u_o = P_{ob}u - Ny \qquad u_o \in \Re^{nc} \tag{5}$$

$$u = -H^o z_{ob} \tag{6}$$

where P_{ob} and N are free parameter matrices of compatible dimensions. The matrices P^o_{ob} and H^o are predetermined by the choice of observability indices ν_i, and their structure is given as

$$P^o_{ob} = \text{block diag}[P^o_1, \ldots, P^o_m] \tag{7}$$

$$P^o_i \begin{bmatrix} 0 & 0 & & 0 & 0 \\ 1 & 0 & \ldots & 0 & 0 \\ 0 & 1 & & 0 & 0 \\ & & \vdots & & \\ 0 & 0 & & 0 & 0 \\ & & \cdots & & \\ 0 & 0 & & 1 & 0 \end{bmatrix}_{\nu_i \times \nu_i} \tag{8}$$

$$H^o = \text{block diag}\,\{[0, \ldots, 0\;\; 1]_{1\times\nu_i}\,, i = 1, \ldots, m\} \tag{9}$$

The observability indices are subject to the following constraints:

$$\sum_{i=1}^{m} \nu_i = nc \tag{10}$$

$$\nu_i \leq \nu_i + 1 \tag{11}$$

The compensator transfer function $K_{ob}(s)$ from y to u is

$$K_{ob}(s) = H^o(sI - P)^{-1}N \tag{12}$$

where

$$P = P^o_{ob} - P_{ob}H^o \tag{13}$$

Note that this compensator structure is constrained to be strictly proper. The advantage of this canonical form is that the design of the free parameter matrices reduces to a constant gain output feedback problem when the plant dynamics are adjoined with the compensator dynamics.

Approximate Loop Transfer Recovery at the Plant Input

In Ref. 1, an approximate LTR method is presented for recovery of loop properties at the plant input. This formulation is based on a performance index that penalizes the difference between two closed-loop return signals, corresponding to v_1 and v_2 in Fig. 1. These signals are produced by identical uniformly distributed impulses injected at w_d for zero initial conditions. It has been shown that if $v_2 \to v_1$, then $K_{ob}G$ approximates $K_c\Phi B$ (Ref. 4).

If the compensator is defined using the observer form, then the error signal is given by

$$e_1 = v_1 - v_2 = K_c x - H^o z_{ob} \tag{14}$$

where the full state gain K_c is designed for desirable loop properties at the plant input. In this context, it can be seen from Eq. (14) that the observer form has the unique advantage in that H^o is a predefined matrix. The approximate LTR performance index is

$$J = E_{x_o}\left\{\int_0^\infty \left[e_1^T e_1 + \rho u_o^T u_o\right] \mathrm{d}t\right\} \tag{15}$$

where $E\{x_o x_o^T\} = BB^T$. As the parameter $\rho \to 0$, then $K_{ob}G$ approximates $K_c\Phi B$ to varying degrees depending on the order of the compensator. This problem can be reduced to a standard constant gain output feedback design formulation wherein the plant and compensator state weighting matrices, and the resulting distribution on initial conditions (due to the impulsive inputs), are uniquely defined.[1]

Approximate Recovery of H_∞ Transfer Function Properties

In this section, the methodology for the approximate recovery of H_∞ transfer function properties is developed. First, the transfer functions of both the full state H_∞ design and the dynamic compensator design are analyzed, which then defines the appropriate minimization problem. Next, the design technique is presented as a constant gain output feedback problem where the quadratic performance index weighting matrices are uniquely defined.

Transfer Function Analysis

In Ref. 4, a theorem is presented that justifies the intuitive argument used to develop the approximate LTR technique. This analysis demonstrates that the approximate recovery of loop shapes at the plant input is accomplished by minimizing the performance index in Eq. (15). Several theorems are presented that parallel the analysis in Ref. 4. Specifically, these theorems show that the

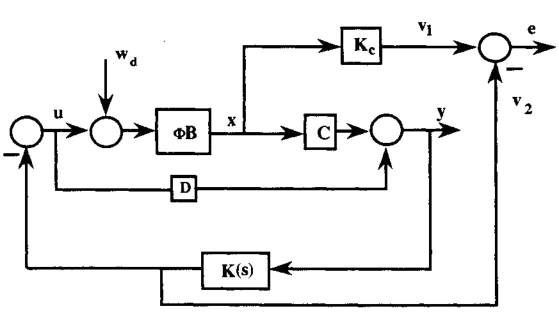

Fig. 1 Approximate LTR formulation for recovery at the plant input.

approximate LTR formulation can be used to approximately recover the H_∞ closed-loop transfer function properties from disturbances to controlled outputs, as long as the system is sufficiently excited.

Theorem 1, responses to w_d. Consider the system shown in Fig. 2 with $w = 0$ and w_d composed of impulses whose strengths are uniformly distributed on the unit ball. Assume that both K_∞ and $K(s)$ are internally stabilizing compensators and that $K(s)$ is strictly proper. If $v_1 = v_2$, then $K(s)G_{22}(s) = K_\infty \Phi B_2$.

Proof: It can be easily verified that

$$u = [I + K(s)G_{22}(s)]^{-1} w_d \tag{16}$$

Thus, the transfer function from w_d to v_2 is given by

$$v_2 = K(s)G_{22}(s)[I + K(s)G_{22}(s)]^{-1} w_d \tag{17}$$

and the transfer function from w_d to v_1 is

$$v_1 = K_\infty \Phi B_2 [I + K(s)G_{22}(s)]^{-1} w_d \tag{18}$$

Using the assumption that $v_1 = v_2$, then

$$e = v_1 - v_2 = G_e w_d = 0 \tag{19}$$

where

$$G_e = [K_\infty \Phi B_2 - K(s)G_{22}(s)][I + K(s)G_{22}(s)]^{-1} \tag{20}$$

If $w_{d_i} = a_i \delta$, where $E\{a_i a_j\} = 1$ for $i = j$ and 0 otherwise, then

$$E\left\{\int_0^\infty e^T e \, \mathrm{d}t\right\} = \frac{1}{2\pi}\int_{-\infty}^{\infty} \mathrm{tr}\,[G_e^*(j\omega) G_e(j\omega)]\,\mathrm{d}\omega = 0 \tag{21}$$

It follows from Eqs. (19–21) that

$$K(s)G_{22}(s) = K_\infty \Phi B_2 \tag{22}$$

□

Letting e_i be the error signal corresponding to $w_{d_i} = a_i \delta$, then the H^2 norm of G_e is

$$\|G_e\|_2^2 = E\left\{\sum_i \|e_i\|_2^2\right\} = E\left\{\int_0^\infty e^T e \, \mathrm{d}t\right\} \tag{23}$$

By minimizing the H_2 norm of the error signal, $\|G_e\|_2$ is minimized, and thus $K(s)G_{22}(s)$ approximates $K_c \Phi B_2$. Note from Eq. (20) that G_e is $[K_c \Phi B_2 - K(s)G_{22}(s)]$ scaled by the sensitivity function $[I + K(s)G_{22}(s)]^{-1}$. This has the effect of normalizing the error signal to the loop gain up to the gain crossover frequency. Since both $K_c \Phi B_2$ and $K(s)G_{22}(s)$ are small at high frequency, errors at these frequencies are not as significant. They lie outside the control bandwidth. At high frequency, the sensitivity function is also small (near identity) in comparison to the loop gain at low frequency and provides a smaller weight to the high frequency error.

Theorem 2, responses to w and w_d. Consider the system shown in Fig. 2 with $\mathcal{W}^T = [w_d^T, w^T]$ composed of impulses whose strengths are uniformly distributed on the unit ball. Let K_∞ be an internally stabilizing full state feedback gain and $K(s)$ be an internally stabilizing, strictly proper output feedback controller. If $v_1 = v_2$, then $K(s)G_{21}(s) = K_\infty \Phi B_1$ and $K(s)G_{22}(s) = K_\infty \Phi B_2$.

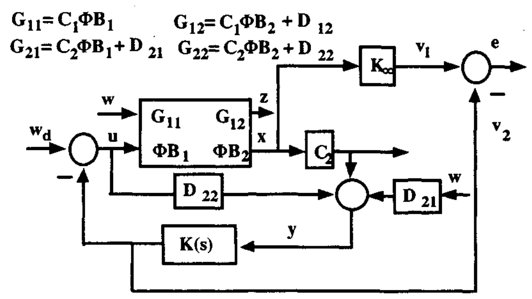

Fig. 2 Formulation to approximately recover T_{zw}.

Proof: In this case, it can be easily verified that the transfer function from $\mathcal{W}$ to v_2 is

$$v_2 = \begin{bmatrix} K(s)G_{22}(s)[I + K(s)G_{22}(s)]\,w \\ I - K(s)G_{22}(s)[I + K(s)G_{22}(s)^{-1}]\; K(s)G_{21}(s)\, w_d \end{bmatrix} \tag{24}$$

Likewise, the transfer function from $\mathcal{W}$ to v_1 is

$$v_1 = \begin{bmatrix} [K_\infty \Phi B_2 [I + K(s)G_{22}(s)]^{-1} w] \\ K_\infty \Phi B_1 - K_\infty \Phi B_2\, [I + K(s)G_{22}(s)]^{-1} K(s)G_{21}(s)\, w_d \end{bmatrix} \tag{25}$$

Under the assumption $v_1(s) = v_2(s)$, then

$$e = v_1 - v_2 = G_e(s)\mathcal{W} = [G_{e_1}(s)\; G_{e_2}(s)]\mathcal{W} = 0 \tag{26}$$

where

$$G_{e_1}(s) = [K_\infty \Phi B_2 - K(s)G_{22}(s)]\,[I + K(s)G_{22}(s)]^{-1} \tag{27}$$

$$G_{e_2}(s) = K_\infty \Phi B_1 - K(s)G_{21}(s) - G_{e_1}(s)K(s)G_{21}(s) \tag{28}$$

If $\mathcal{W}_i = a_i \delta$, where $E\{a_i a_j\} = 1$ for $i = j$ and 0 otherwise, then

$$E\left\{\int_0^\infty e^T e \, \mathrm{d}t\right\} = \frac{1}{2\pi}\int_{-\infty}^{\infty} \mathrm{tr}\,[G_e^*(j\omega) G_e(j\omega)]\,\mathrm{d}\omega = 0 \tag{29}$$

It follows from Eqs. (26–29) that

$$K_\infty \Phi B_1 = K(s)G_{21}(s), \qquad K_\infty \Phi B_2 = K(s)G_{22}(s) \tag{30}$$

□

Theorem 3, recovery of T_{zw}. Let T_{zw}^∞ be the transfer function from the disturbance input w to the performance variable z using the full state controller K_∞. Similarly, let T_{zw}^{dc} be the transfer function from the disturbance input w to the performance variable z using the compensator $K(s)$. Referring to Fig. 2, if $v_1 = v_2$, then $T_{zw}^\infty = T_{zw}^{dc}$.

Proof: It can be shown that

$$T_{zw}^\infty = G_{11} - G_{12}(I + K_\infty \Phi B_2)^{-1} K_\infty \Phi B_1 \tag{31}$$

and

$$T_{zw}^{dc} = G_{11} - G_{12}[I + K(s)G_{22}(s)]^{-1} K(s)G_{21}(s) \tag{32}$$

Using the results of Theorem 2, if $v_1 = v_2$, then

$$K(s)G_{22}(s) = K_\infty \Phi B_2 \tag{33}$$

$$K(s)G_{21}(s) = K_\infty \Phi B_1 \tag{34}$$

and thus

$$T_{zw}^\infty = T_{zw}^{dc} \tag{35}$$

□

The proofs of Theorems 1 and 2 rely on the fact that the system is sufficiently excited by impulsive inputs at w and w_d. In the compensator design methodology to be discussed next, these inputs are equivalently modeled as a distribution of initial conditions. For the plant states, this means that

$$X_o = E\{x_o x_o^T\} = [\bar{B}\,\bar{B}^T], \qquad \bar{B} = [B_1\;\; B_2] \tag{36}$$

However, it is sufficient that the columns of $\bar{B}$ span the column space of $[B_1\, B_2]$. To see this, perform the following decomposition of B_1:

$$B_1 = B_2\mathcal{D} + \delta B_1, \qquad B_2^T \delta B_1 = 0 \tag{37}$$

Substitution of Eq. (37) into the proof of Theorem 2 leads to the conclusion that if $v_1 = v_2$, then

$$K_\infty \Phi \delta B_1 = K(s)\delta G_{21}(s), \qquad K_\infty \Phi B_2 = K(s)G_{22}(s) \tag{38}$$

where $\delta G_{21}(s) = C_2\Phi\delta B_1$. Making the same substitution in the proof of Theorem 3, then

$$T^\infty_{zw} = G_{11} - G_{12}(I + K_\infty\Phi B_2)^{-1}[K_\infty\Phi B_2\mathfrak{D} + K_\infty\Phi\delta B_1] \tag{39}$$

$$T^{dc}_{zw} = G_{11} - G_{12}[I + K(s)G_{22}(s)]^{-1}[K(s)G_{22}(s)\mathfrak{D} + K(s)\delta G_{21}(s)] \tag{40}$$

from which it follows that $T^\infty_{zw} = T^{dc}_{zw}$. The implication of Eq. (40) is that one may choose $\bar{B} = [\delta B_1 \; B_2]$.

Compensator Design Methodology

To formulate the approximate recovery of H_∞ loop properties as a constant gain output feedback problem, consider the state space realization of the system shown in Fig. 2.

$$\begin{Bmatrix} \dot{x} \\ z \\ y \end{Bmatrix} = \begin{bmatrix} A & B_1 & B_2 \\ C_1 & 0 & D_{12} \\ C_2 & D_{21} & D_{22} \end{bmatrix} \begin{Bmatrix} x \\ w \\ u \end{Bmatrix} \qquad \begin{matrix} x \in \Re^n & w \in \Re^{m_1} & u \in \Re^{m_2} \\ z \in \Re^{p_1} & y \in \Re^{p_2} & \end{matrix} \tag{41}$$

The plant and the observer canonical compensator are augmented to form the following system:

$$\dot{\boldsymbol{x}} = \boldsymbol{A}\boldsymbol{x} + \boldsymbol{B}\boldsymbol{u} \qquad \boldsymbol{x} \in \Re^{n+nc}, \quad \boldsymbol{u} \in \Re^{nc} \tag{42}$$

$$\boldsymbol{y} = \boldsymbol{C}\boldsymbol{x} \qquad \boldsymbol{y} \in \Re^{m_2+p_2} \tag{43}$$

$$\boldsymbol{u} = -\boldsymbol{G}\boldsymbol{y} \tag{44}$$

where $\boldsymbol{x}^T = \{x^T, z^T_{\text{ob}}\}$, $\boldsymbol{u} = u_o$ and $\boldsymbol{y}^T = \{y^T, -u^T\}$, and

$$\boldsymbol{A} = \begin{bmatrix} A & -B_2H^o \\ 0 & P^o_{\text{ob}} \end{bmatrix}, \qquad \boldsymbol{B} = \begin{bmatrix} 0 \\ I_{nc} \end{bmatrix} \tag{45}$$

$$\boldsymbol{C} = \begin{bmatrix} C_2 & -D_{22}H^o \\ 0 & H^o \end{bmatrix}, \qquad \boldsymbol{G} = [N \;\; P_{\text{ob}}] \tag{46}$$

Note that the free parameter matrices used in designing the compensator are compactly placed in the equivalent constant gain feedback matrix $\boldsymbol{G}$. The error signal to be penalized is given by

$$e_{\text{ob}} = v_1 - v_2 = K_\infty x - H^o z_{\text{ob}} \tag{47}$$

where the full state gain K_∞ is a full state H_∞ controller.

The approximate LTR performance index is

$$J = E_{x_o}\left\{\int_0^\infty \left[e^T_{\text{ob}}e_{\text{ob}} + \rho u^T_{\text{ob}}u_{\text{ob}}\right](\mathrm{d}t)\right\} \tag{48}$$

Substituting Eq. (47) into Eq. (48), and rewriting the performance index as

$$J = E_{x_o}\left\{\int_0^\infty [\boldsymbol{x}^T Q \boldsymbol{x} + \boldsymbol{u}^T R \boldsymbol{u}]\,\mathrm{d}t\right\} \tag{49}$$

yields the following plant and compensator state weighting matrices:

$$Q = \begin{bmatrix} K^T_\infty K_\infty & -K^T_\infty H^o \\ -H^{oT}K_\infty & H^{oT}H^o \end{bmatrix}, \qquad R = \rho I_{\text{nc}} \tag{50}$$

The effect of an impulse distribution at both the control and disturbance inputs may be modeled as a distribution of initial conditions. For the case $D_{21} = 0$, the corresponding initial covariance matrix is given as

$$\mathrm{E}\{\boldsymbol{x}_o \boldsymbol{x}^T_o\} = \boldsymbol{X}_o = \begin{bmatrix} \bar{B}\bar{B}^T & 0 \\ 0 & 0 \end{bmatrix}, \qquad \bar{B} = [B_1 \;\; B_2]W \tag{51}$$

where W is used to individually weight the impulse strengths. As noted earlier, it is only required that $\bar{B}$ span the column space of $[B_1 \; B_2]$.

Equations (42–44) and (49) constitute a constant gain output feedback problem whose necessary conditions for optimality are well known.[12] As the parameter $\rho \to 0$, then of the compensator approximates T^∞_{zw} of the full state H_∞ controller to varying degrees depending on the order of the compensator. Note that the compensator design procedure permits the case $D_{21} = 0$ (or more generally rank deficient) whereas the Riccati equation approaches of Refs. 5 and 8 require D_{21} to be full rank.

Effect of D_{21} Term on the Design Methodology

If disturbances are introduced at the plant output, then $D_{21} \neq 0$. In effect, these output disturbances produce a nonzero initial condition distribution on the compensator states. Two techniques are discussed next that address the implications of this issue on the design methodology. The solution for K_∞ in the full state feedback design step is independent of D_{21}.

The first technique accounts for the nonzero initial condition distribution on the compensator states. If $D_{21} \neq 0$, then the $\boldsymbol{X}_o$ matrix is given by

$$\boldsymbol{X}_o = \begin{bmatrix} \bar{B}\bar{B}^T & 0 \\ 0 & ND_{21}D^T_{21}N^T \end{bmatrix} \tag{52}$$

Now, $\boldsymbol{X}_o$ is dependent on N, which is an unknown free parameter matrix. Using the definitions in Eqs. (42–46), Eq. (52) can be rewritten as

$$\boldsymbol{X}_o = \boldsymbol{X}_{o_1} + \boldsymbol{B}\boldsymbol{G}\boldsymbol{X}_{o_2}\boldsymbol{G}^T\boldsymbol{B}^T \tag{53}$$

where

$$\boldsymbol{X}_{o_1} = \begin{bmatrix} \bar{B}\bar{B}^T & 0 \\ 0 & 0 \end{bmatrix}, \qquad \boldsymbol{X}_{o_2} = \begin{bmatrix} D_{21}D^T{}_{21} & 0 \\ 0 & 0 \end{bmatrix} \tag{54}$$

Since Eq. (53) is a function of $\boldsymbol{G}$, the standard necessary conditions for optimal output feedback[12] no longer apply. The new necessary conditions for optimality are given in Ref. 13.

A second approach addressing $D_{21} \neq 0$ involves the introduction of a dynamic filter in each output channel that prevents a direct feedthrough of disturbances to outputs; and thus, once the filter is augmented with the generalized plant, $D_{21} = 0$. The filters are used solely for the compensator design step and are not implemented in the controller. This approach is demonstrated in the second design example.

Design Examples

Example 1: Inverted Pendulum and Cart

The first design example is a simple inverted pendulum and cart, Fig. 3. This example demonstrates a straightforward application of

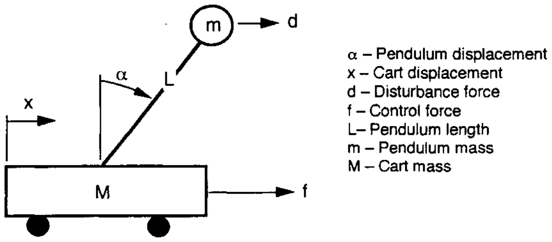

Fig. 3 Inverted pendulum and cart system.

the compensator design methodology. The control force f acts on the cart, and a disturbance force d acts on the pendulum mass. For this system, the equations of motion are given in Eq. (55).

$$\begin{Bmatrix} \dot{x} \\ \dot{\alpha} \\ \ddot{x} \\ \ddot{\alpha} \end{Bmatrix} = \begin{bmatrix} 0 & 0 & 1 & 0 \\ 0 & 0 & 0 & 1 \\ 0 & -mg/M & 0 & 0 \\ 0 & (M+m)g/ML & 0 & 0 \end{bmatrix} \begin{Bmatrix} x \\ \alpha \\ \dot{x} \\ \dot{\alpha} \end{Bmatrix}$$

$$+ \begin{bmatrix} 0 & 0 \\ 0 & 0 \\ -1/M & 1/M \\ 1/ML + 1/ML & -1/ML \end{bmatrix} \begin{Bmatrix} d \\ f \end{Bmatrix} \tag{55}$$

where α is the pendulum angular displacement and x is the cart displacement. The outputs of this system are chosen to be $y = \{x, \alpha, \dot{\alpha}\}$ and $z = \{y^t, u\}$. For purposes of this example, the following dimensions are assumed: $L = 0.3048$ m, $m = 0.2268$ kg, and $M = 1.361$ kg. The disturbance force is scaled by 0.1, and then a full state feedback controller is computed such that

$$\|T_{zw}\|_\infty \leq 1.0 \tag{56}$$

The resulting feedback gains are given as

$$K_\infty = [-5.8834 \ -128.7326 \ -11.6251 \ -21.4931] \tag{57}$$

A third-order compensator is selected for this example. A single compensator index, $\nu = 3$, is allowable for this system. With $\bar{B}$ equal to the input matrix in Eq. (55), the dynamic compensator design approximately recovers T_{zw}^{∞} as ρ is reduced in Eq. (48). The compensator free parameter matrices are computed using a convergent sequential algorithm.[14] In Fig. 4, it is observed that the recovery of T_{zw}^{∞} is achieved for the $\rho = 1.0E-7$ design. The resulting free parameter matrices for this design are given in Eq. (58).

$$N = \begin{bmatrix} 622.70 & 14{,}587.0 & 2403 \\ 4673.5 & 88{,}096.0 & -1113.8 \\ 7977.7 & 43{,}842.0 & 5431.5 \end{bmatrix}, \quad P_{\mathrm{ob}} = \begin{bmatrix} 100.48 \\ -8.7627 \\ 291.33 \end{bmatrix} \tag{58}$$

The large values are characteristic of loop transfer recovery (even in the full order case) in that some of the compensator poles approach infinity and the parameter ρ is reduced. In practice, ρ should be adjusted so that adequate recovery is achieved while avoiding presence of high frequency modes in the compensator. This will be illustrated in the next example.

Example 2: Longitudinal Flight Controller for the F-18

The F-18/HARV four state linearized longitudinal dynamical model is given in Refs. 10 and 11 for a low speed, high angle of attack (Mach 0.24, $\alpha = 25$ deg) at 15,000-ft altitude. This flight condition is considered to be a difficult trim point. The state space representation of the dynamics is given by

$$\dot{\mathcal{X}} = \mathcal{A}\mathcal{X} + \mathcal{B}u \tag{59}$$

where the scaled system matrices are

$$\mathcal{A} = \begin{bmatrix} -0.0750 & -0.1399 & 0 & -0.1871 \\ -0.1517 & -0.1959 & 0.9896 & 0 \\ -0.0258 & -0.1454 & -0.1877 & 0 \\ 0 & 0 & 1.0 & 0 \end{bmatrix} \tag{60}$$

$$\mathcal{B} = \begin{bmatrix} -0.3830 & 0 & -0.8258 & 0.0262 & -0.4114 & 1.4400 \\ -0.5157 & -0.3224 & -0.8377 & -0.0054 & -0.5157 & -0.4641 \\ -19.141 & -2.0054 & -23.3767 & -0.0653 & 1.2032 & 0.7271 \\ 0 & 0 & 0 & 0 & 0 & 0 \end{bmatrix} \tag{61}$$

and the state and control vectors are

$$\mathcal{X} = \begin{Bmatrix} \text{true airspeed } v^T, \ 1/8 \text{ ft/s} \\ \text{angle of attack } \alpha, \text{ deg} \\ \text{pitch rate, rad/s} \\ \text{pitch angle, deg} \end{Bmatrix}$$

$$u = \begin{Bmatrix} \text{symmetric thrust vectoring vane, deg} \\ \text{symmetric aileron, deg} \\ \text{symmetric stabilator, deg} \\ \text{symmetric leading-edge flap, deg} \\ \text{symmetric leading-edge flap, deg} \\ \text{throttle position, deg} \end{Bmatrix} \tag{62}$$

This model has an unstable phugoid mode at $0.0188 \pm 0.1280j$ and a stable short period mode at $-0.248 \pm 0.3585j$.

Three of the six control inputs are redundant since rank $(\mathcal{B}) = 3$. Following the procedure in Refs. 10 and 11, the actual system, Eq. (59), can be replaced by the pseudosystem

$$\dot{\mathcal{X}} = \mathcal{A}\mathcal{X} + B_v v \tag{63}$$

where v is a vector of three linearly independent pseudocontrols and B_v spans the column space of $\mathcal{B}$. Accounting for the structure of $\mathcal{B}$, an appropriate choice for B_v is

$$B_V = \begin{bmatrix} I_3 \\ 0 \end{bmatrix} \tag{64}$$

A controller can now be designed using the pseudosystem, and as a postdesign step, the pseudocontrols can be mapped onto the actual controls. This transformation is given by

$$u = T_v \tag{65}$$

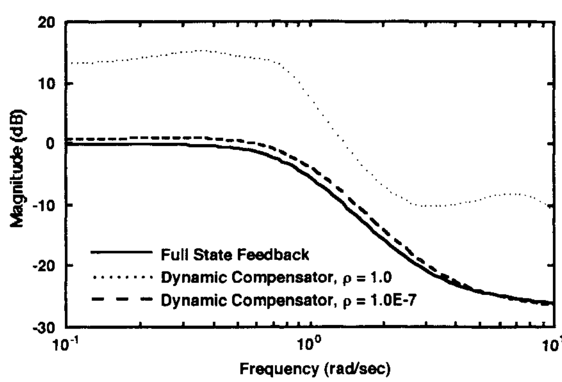

Fig. 4 Approximate recovery of T_{zw} for example 1.

where

$$T = \mathcal{W}^{-1} B_1^T (\mathcal{B}_1 \mathcal{W}^{-1} B_1^T)^{-1}, \qquad \mathcal{W} = \mathrm{diag}\{1 \;\; 1 \;\; 1 \;\; 1 \;\; 1.3 \;\; 1\} \quad (66)$$

and $\mathcal{B}_1$ is the upper 3×6 block of $\mathcal{B}$. This transformation distributes the pseudocontrols so that the weighted energy of the actual redundant controls is minimized. This approach also provides for reconfigurable control. The details of this optimization procedure are given in Ref. 11.

Generalized Plant and Dynamic Compensator Design

The generalized plant for this design is shown in Fig. 5, where $\Phi = (sI - \mathcal{A})^{-1}$. Note that the disturbances w are injected at the plant output. The plant outputs are v_T, γ, θ, and p, where $\gamma = \theta - \alpha$. To ensure type I behavior, three integrators are introduced into the system dynamics. The performance variables are selected as $z^T = \{\lambda^T, g_1\int v_T, g_1\int\gamma, g_1\int\theta, v^T\}$, where λ is the output of the W_λ filter given as

$$W_\lambda(s) = \frac{g_2}{s^2 + 2\zeta\omega s + \omega^2} I_{3\times 3}, \quad \omega = 10 \text{ rad/s}, \quad \zeta = 1.0 \quad (67)$$

The gains on the integrator states and the W_λ filter are used to adjust the bandwidth of the full state controller design. The filter $W_y(s)$ is introduced to prevent a direct feedthrough from disturbances to outputs. For this design, the filter pole is set at -5 rad/s for each output. Note that in this case the proportional plus integral structure is created external to the actual compensator design by treating the integrated quantities as measurements. This means that the integrators will be implemented as part of the final controller design.

A state space representation for the generalized plant can be realized in the form of Eq. (41). By setting $g_1 = g_2 = 0.625$ and scaling w by 0.125, a full state H_∞ controller is first designed so that

$$\|T_{zw}\|_\infty \le \gamma_1 = 1.75 \quad (68)$$

This value of γ_1 is slightly lower than the value used for the output feedback H_∞ design in Refs. 10 and 11.

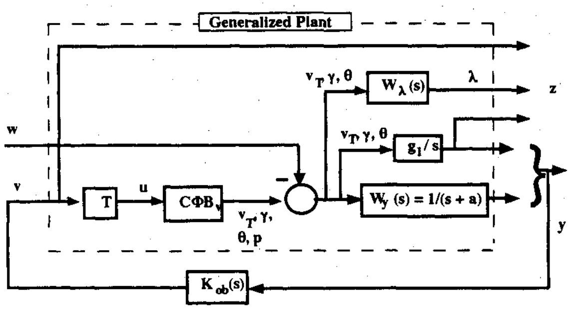

Fig. 5 Generalized plant for the F-18 dynamic compensator design.

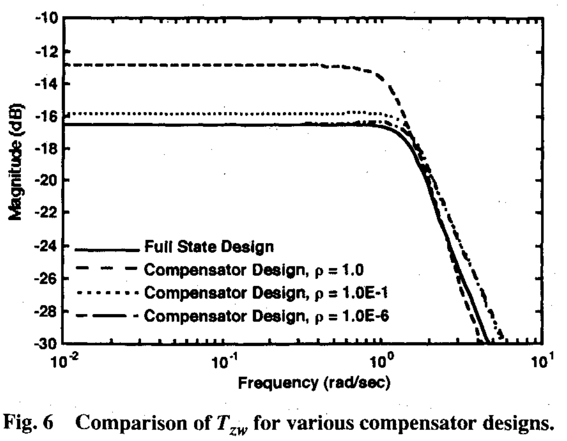

Fig. 6 Comparison of T_{zw} for various compensator designs.

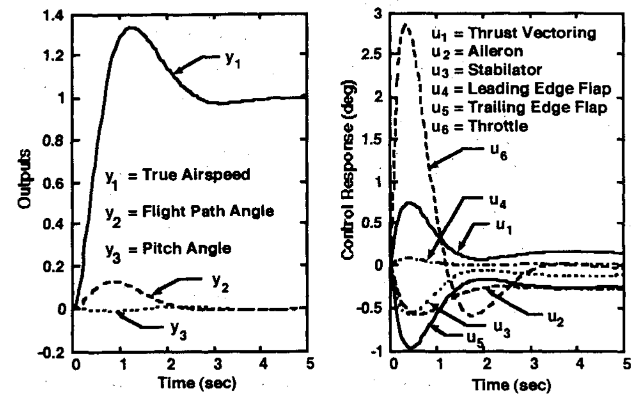

Fig. 7 System response to a v_T step command.

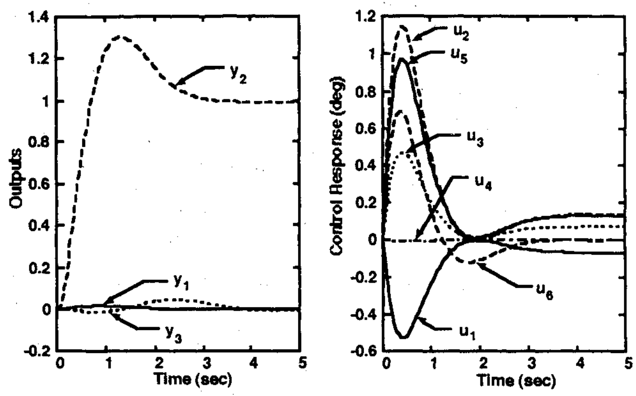

Fig. 8 System response to a γ step command.

A third-order observer form dynamic compensator is selected to recover the properties of the H_∞ full state controller. The X_o matrix in Eq. (51) is constructed with $\bar{B} = [B_1 \; B_2]$. In Fig. 6, the maximum singular value of T_{zw} is compared for the full state design and several dynamic compensator designs. Note that as ρ is reduced from $\rho = 1.0$ to $\rho = 1.0E-6$, the recovery of the full state T_{zw} properties improves. For the full state design, $\|T_{zw}\|_\infty = -16.49$ dB and for the $\rho = 1.0$, $1.0E-1$ and $1.0E-6$ designs, $\|T_{zw}\|_\infty = -12.83$ dB, -15.80 dB, and -16.35 dB, respectively. However, as ρ is reduced, the compensator modes become fast. Considering the tradeoff between recovery and natural frequency of the compensator modes, the $\rho = 1.0E-1$ design is selected as the most desirable. For this design, the compensator free parameter matrices are given as

$$N = \begin{bmatrix} 36.10 & 0.799 & -2.021 & -0.559 & 3.163 & -0.001 & 0.007 \\ -2.226 & -12.52 & 7.725 & 2.392 & 0.003 & 3.103 & -0.610 \\ -0.965 & -1.327 & 23.92 & 15.59 & -0.007 & 0.610 & 3.104 \end{bmatrix} \quad (69)$$

$$P_{ob} = \begin{bmatrix} -6.0880 & 0.1344 & 0.0704 \\ -0.1344 & -5.9111 & -0.3013 \\ 0.0704 & -0.3013 & -6.4110 \end{bmatrix} \quad (70)$$

In Figs. 7–9, the time response to step commands in v_T, γ, and θ are shown. In each response, the 90% settling time is near 5 s, which is considered acceptable. Except for u_6 in Fig. 7 and u_2 in Fig. 8, all control deflections are less than 1.0 deg.

Comparison with a Full- and Reduced-Order H_∞ Design

Figures 10 and 11 show the result of a full-order H_∞ design performed using the two Riccati equation approach of Ref. 5, with γ_1

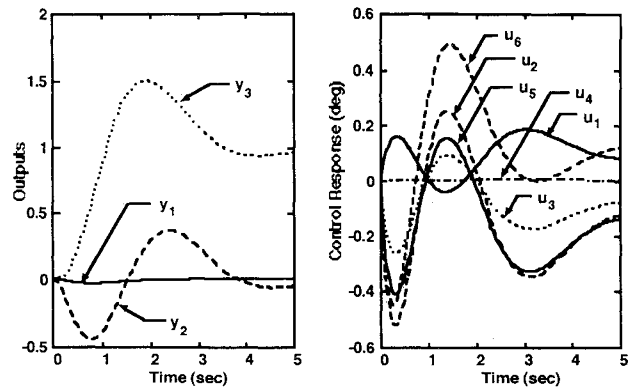

Fig. 9 System response to a θ step command.

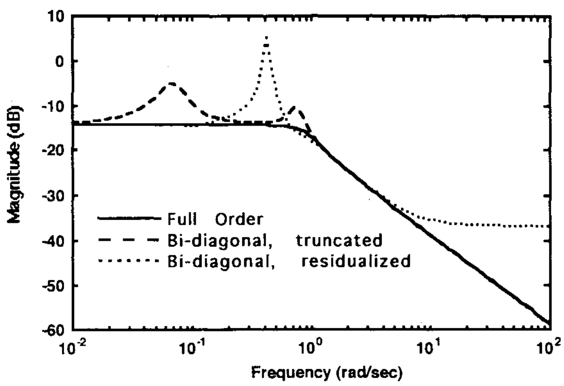

Fig. 10 T_{zw} for full-order and bidiagonal reduced-order controllers.

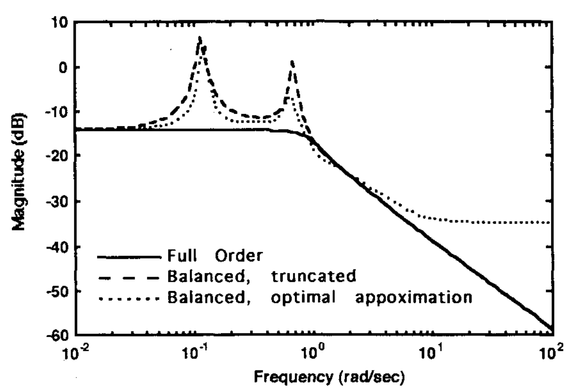

Fig. 11 T_{zw} for full-order and balanced realization reduced-order controllers.

= 1.75. The generalized plant is identical to that of Fig. 6 with the exception that the integrated states are not available for feedback and the $W_y(s)$ filters are deleted (to ensure that D_{21} is full rank). In this design, the resulting compensator achieves proportional plus integral control internally as a consequence of the integral weighting in the performance variable z. The compensator is strictly proper and requires 13 state variables in its realization. A comparison of Figs. 6 and 10 demonstrates that the fixed-order compensator and the full order controller provide similar robustness properties as measured by the infinity norm.

Figures 10 and 11 also illustrate what occurs to the maximum singular value plot when the order of the compensator is reduced using a variety of methods. In each case, the dimension of the controller was reduced to six to match the dimension of the controllers in the fixed-order results of Fig. 6 (third-order compensator plus three external integrators). The infinity norm of the full-order controller is −14.18 dB.

The reduced-order controllers were obtained using the options available in MATLAB/μ-tools.[15] In Fig. 10, the system was first transformed to bidiagonal form (strans) and then either truncated (strunc) or residualized (sresid). The residualized controller is proper. In Fig. 11, a balanced realization was first obtained using Hankel singular values (sysbal), followed by truncation (strunc) or by computing an optimal Hankel norm approximation (hankmr). The controller for this last option is again proper. In addition, five variations of these approaches were tried, all of which gave similar results. In each case, the infinity norm for the reduced-order controller was significantly higher than that of the full-order controller and the fixed-order controllers of Fig. 6. This illustrates the fact that the objective functions used in obtaining reduced-order controllers are not compatible with the original design objective.

Conclusions

This paper has developed an approximate loop transfer recovery technique for designing fixed-order dynamic compensators. This methodology is used to approximate the loop properties of an H_∞ full state controller. This technique is based upon a unique selection of the quadratic performance index weighting matrices and the initial condition matrix.

Two examples are presented to demonstrate this design technique. The first example is a simple inverted pendulum and cart system. The second example is a longitudinal flight controller for the F-18 fighter aircraft. In both examples, the fixed-order dynamic compensator provides nearly the same infinity norm as the full state feedback design. The second example demonstrates that the process of full-order design followed by controller-order reduction can lead to significantly degraded performance and measured by the infinity norm. This has significant implications in design for robust performance since minimizing an infinity norm is a crucial step in satisfying robust performance specifications in both H_∞ design and in μ-synthesis.

Acknowledgments

The authors would like to thank Harold Buschek of Georgia Institute of Technology for his contribution to this paper. Buschek produced the full-order and reduced-order controller designs used for comparison with the fixed-order results in example 2. This research was supported by the Army Research office under contract number DA A603-88C-0003.

References

[1]Calise, A. J., and Prasad, J. V. R., "An Approximate Loop Transfer Recovery Method for Designing Fixed Order Compensators," *Journal of Guidance, Control, and Dynamics,* Vol. 13, No. 2, 1990, pp. 297–302.

[2]Kramer, F. S., and Calise, A. J., "Fixed Order Dynamic Compensation for Multivariable Linear Systems," *Journal of Guidance, Control, and Dynamics,* Vol. 11, No. 1, 1988, pp. 80–85.

[3]Doyle, J. C., and Stein, G., "Multivariable Feedback Design: Concepts for a Classical/Modern Synthesis," *IEEE Transactions on Automatic Control,* Vol. AC-26, Feb. 1981, pp. 4–16.

[4]Calise, A. J., and Byrns, E. V., Jr., "Output Loop Transfer Recovery for Fixed Order Dynamic Compensators," American Control Conference, San Diego, CA, May 1990; also *Optimal Control Theory and Applications* (to be published).

[5]Doyle, J. C., Glover, K., Khargonekar, P. P., and Francis, B. A., "State Space Solutions to Standard H_2 and H_∞ Control Problems," *IEEE Transactions on Automatic Control,* Vol. AC-34, Aug. 1989, pp. 831–847.

[6]Petersen, I. R., "Disturbance Attenuation and H_∞ Optimization: A Design Method Based on the Algebraic Riccati Equation," *IEEE Transactions on Automatic Control,* Vol. AC-32, May 1987, pp. 427–429.

[7]Petersen, I. R., "Disturbance Attenuation: A Design Method Based on the Algebraic Riccati Equation," Third Conference on Control Engineering, Sydney, Australia, May 1986.

[8]Bernstein, D. S., and Haddad, W. M., "LQG Control with an H_∞ Performance Bound: A Riccati Equation Approach," *IEEE Transactions on Automatic Control,* Vol. AC-34, March 1989, pp. 293–305.

[9]Hyland, D. C., and Bernstein, D. S., "The Optimal Projection Equations

for Fixed Order Dynamic Compensation," *IEEE Transactions on Automatic Control,* Vol. AC-29, Nov. 1984, pp. 1034–1037.

[10]Voulgaris, P., and Valavani, L., "High Performance H_2 and H_∞ Designs for the Supermaneuverable F-18/HARV Fighter Aircraft," *Journal of Guidance, Control, and Dynamics,* Vol. 14, No. 1, 1991, pp. 157–165.

[11]Voulgaris, P., "High Performance Multivariable Control of the 'Supermaneuverable' F18/HARV Fighter Aircraft," M.S. Thesis, Dept. of Aeronautics and Astronautics, Massachusetts Inst. of Technology, Boston, MA, May 1988.

[12]Mendel, J. M., "A Concise Derivation of Optimal Constant Limited State Feedback Gains," *IEEE Transactions on Automatic Control,* Vol. AC-19, Aug. 1974, pp. 447, 448.

[13]Byrns, E. V., Jr., "Design and Analysis of Robust Fixed Order Dynamic Compensators," Ph. D. Dissertation, School of Aerospace Engineering, Georgia Institute of Technology, Atlanta, GA, May 1991.

[14]Moerder, D. D., and Calise, A. J., "Convergence of a Numerical Algorithm for Calculating Optimal Output Feedback Gains," *IEEE Transactions on Automatic Control,* Vol. AC-30, Sept. 1985, pp. 900–903.

[15]Balas, G. J., et. al., "µ-Analysis and Synthesis Toolbox, User's Guide," MUSYN Inc., Minneapolis, MN, April, 1991, pp. 35–46.